Transient Diffusion of Nanovectors in Permeable Capillaries

F. Gentile[1], M. Ferrari[2, 3], P. Decuzzi[1, 2]

[1] BioNEM - Center of Bio/Nanotechnology and Engineering for Medicine
University of Magna Graecia at Catanzaro Viale Europa, 88100 Catanzaro, ITALY
[2] The University of Texas Health Science Center
1825 Pressler, Suite 537D, Houston, TX 77031
[3] M.D. Anderson Cancer Center and Rice University
Houston - Texas - 77030

Abstract

The strategy currently followed to deliver nano-sized particulates to solid tumors is based on the well known enhanced permeability and retention effect where particles sufficiently small to spontaneously extravasate through the fenestrated tumor vessels can be transported from the vascular compartment to the inner region of the tumor mass and from there release their payload. An alternative active strategy is gaining consensus and is based on the targeting of the tumor vasculature through ligand-receptor specific interactions exploiting the biological and biophysical differences between normal and tumor vessel walls. Such an active strategy requires a detailed analysis of the transport and adhesive interaction of nano-sized particulate systems within the tumor vasculature which is characterized by permeable walls; high interstitial fluid pressure; and expression of specific receptor molecules.

In this work, the analysis of the transport of solute molecules resembling nano-sized particles under laminar flow is presented solving the classical diffusion-advection equation in a straight capillary. The effect of vessel wall permeability as well as the complex rheological behavior of blood are considered explicitly keeping the formulation tractable. Possible future directions of research are then presented in the closing paragraph where a finite element approach is described to treat the transport of non- conventional particulate systems having a non spherical shape.

Key words: transient diffusion, permeable vessels, nanovectors, drug delivery.

1. Introduction

Small-molecule agents and monoclonal antibodies (mAbs) as well as particulate formulations have been developed, subjected to clinical trials and some are already employed in the clinics to cure cancer. Despite this, the vast majority of malignancies have proven to be resistant to such interventions, partially due to the requisite dose limitations for preventing adverse effects on normal tissues but largely due to the barriers of different nature that these systemically administered agents should avoid before reaching their biological target (Minchinton and Tannock [1]; Ferrari [2]).

It is reported that small-molecules and therapeutic antibodies reach the desired biological target only in 1 part per 10,000-100,000 molecules (Li et al. [3]). Most of these molecules are lost within the body, in that for their small size (<1-5 nm) they can easily cross the endothelial barrier and diffuse through the extracellular matrix of almost any normal tissue. Others are eliminated from the blood pool through the action of the immune system. And those that reach the tumor vasculature are prevented from penetrating deep in the tumor mass by the adverse interstitial fluid pressure and by the composition and highly intricate structure of the extracellular matrix of tumors (Heldin et al. [4]). The transport of nano-sized molecules and particulate systems within capillaries with permeable walls, as is the case of tumors, and in the presence of blood cells altering significantly the rheological properties of the hosting fluid is of vital importance in the design and development of such particulate systems, and this is one of the most active field of research in Cancer NanoTechnology.

General. Taylor (1953) first studied the effect of shear on axial dispersion in fully developed laminar flow of a Newtonian fluid in a circular tube. A similar solution is readily obtained for the flow between plates. To introduce the concept of shear-augmented dispersion, consider a bolus of a passive species in fully developed incompressible laminar Newtonian flow in a straight channel. The bolus is carried downstream by the Poiseuille flow. At the leading edge of the bolus, the solute diffuses from the high concentration region near the center of the tube toward the low concentration region at the wall. In doing so, the amount of material travelling at a speed greater than the average is reduced, thereby reducing the rate of axial spread of the bolus relative to its axial center, which moves with the cross-sectional average velocity. At the trailing edge, diffusion is inward, again reducing the variance of the velocity of the bolus. The non-uniform flow stretches the species concentration profile along the capillary generating transverse variations in concentration, which are destroyed by transverse molecular diffusion reshaping the concentration profile. This mechanisms results in an effective diffusion coefficient D_{eff} that for a laminar flow in a circular pipe of radius R_e with non permeable walls has been derived as (Aris [6]):

$$D_{eff} = D_m + \frac{V \mathrm{R_e}}{48 D_m} \tag{1}$$

Dispersion is maximized as the molecular diffusivity goes to zero since any radial diffusion reduces the axial spread of the material: equation (1) predicts that D_{eff} goes to zero as D_m~0, but in this limit the assumption of small radial concentration gradients breaks down and the result is no longer valid. In contrast to the basis for the Taylor results, the transport becomes purely convective.

Assumptions implicit in this analysis are: (i) the dispersion is quasi-steady, thereby eliminating the temporal term from the species transport equation; (ii) an assumption of unidirectional, usually fully developed, flow eliminates all convective terms except the axial one; (iii) axial convection is dominant over axial diffusion, and (iv) radial variations in concentration are small compared with those in the longitudinal direction. Considerable effort has been expended in attempts to relax Taylor's assumptions. The first assumption can be particularly troublesome, since in a problem involving the spread of a tracer introduced into the flow stream in some arbitrary configuration, the analysis is restricted to the limit of large time. Specifically, the Taylor and Aris (1956) analysis is valid for $t \square ½\ R_e^2/D_m$ that, given particular values of diffusivity and outer diameter describing common physiological conditions, can be also significantly big (considering the dispersion of sub-micrometric particles, with a molecular diffusivity D_m typically ranging between 10^{-11} and 10^{-9} m^2/s, it follows that the Taylor–Aris asymptotic solution is strictly valid in large vessels (arteries) with R_e~10^{-2} m at times larger than 10^5–10^7 s, whereas in small capillaries with R_e~10^{-6} m at times larger than 10^{-3} to 10^{-1} s. Observing that blood in large vessels has a mean velocity V of about 10^2 mm/s, the Taylor–Aris

regime would be fully developed in arteries only after 10^4 *m*. In small capillaries with *V* of about 1 *mm*/*s*, the asymptotic solution would hold true after 10^{-3} to 10^{-1} *mm*, which is smaller than the characteristic length of normal capillaries typically ranging between 100 μm and few millimeters. The analysis carried so far is incomplete to the extent that (i) the permeability of the vessels where dispersion takes place is not considered and (ii) the transient time of dispersion is disregarded, and the solution is given in terms of mean concentration (the radial distribution of concentration cannot be deducted from the mono dimensional analysis of Taylor/Aris).

Ananthakrishnan et al. [5] solved numerically the complete convective-diffusion equation describing the dispersion of the solute within a cylindrical steady laminar flow and observed a perfect agreement with the approximate results of the Taylor & Aris theory in the limit of sufficiently large times t ($t \gg R_e^2/D_m$, as widely reported above). Gill [16] extended Taylor's framework to obtain the local concentration distribution, by means of a series expansion about the mean concentration, while Gill and Sankarasubramanian [16] established that the above-mentioned method of series solution (known as the Generalized Dispersion Model) could exactly reproduce the centroid and the width of the concentration for all time, by solving the following simplified convective-diffusive equation

$$\frac{\partial C_m}{\partial t} = \sum_{i=1}^{\infty} K_i(t) \frac{\partial^i C_m}{\partial z^i} \tag{2}$$

provided that the coefficients of the models $K_i(t)$ are chosen as suitable functions of time. Sankarasubramanian and Gill [22] elaborated the Generalized Dispersion Model (GDM) by including the effects of interphase mass transfer (i.e. by removing the hypothesis of impermeability of the walls to the solute; in such a circumstance, summation in (2) would start from i=0).

Biomedical Applications. In biomedical applications, macromolecules and nanoparticles are systemically administered and transported within capillaries with different radii, lengths and properties. Depending on the organ, the capillary walls can be impermeable, as for the blood-brain endothelium, or can be highly permeable, as for the capillary of the kidney or those of developing tumor masses. In addition to this, the velocity profile in capillaries can be significantly different from parabolic (Poiseuille flow), because of the presence of red blood cells, which tend to accumulate in a central 'core' region of the capillary leaving a marginal 'cell free layer'. In arterioles and venules, the blood velocity profile follows quite accurately the Casson law with a central plug region (zero radial velocity gradient) of radius r_c (plug radius) and an outer region with a parabolic velocity profile.

The velocity profile as well as the wall permeability have a significant effect on the convective transport of a solute. In 1993, Sharp derived explicit expressions for D_{eff} considering non-Newtonian fluids with different rheological laws, namely for a Casson, Bingham plastic, and power-law fluid. In particular, for a Casson fluid, it was determined.

Dash et al. [8] and Nagarani et al. [20] used the Sharp Model in conjunction with the Generalized Dispersion Model to investigate the effects of yield stress (or equivalently the plug radius) and of the irreversible solute-reaction mechanism at the flow boundaries on the dispersion in a Casson fluid through a conduit. In this scenario, the entire phenomenon of solute propagation was described in terms of three effective transport coefficients, that are exchange (K_0, that arises due to adsorption mechanisms at the walls, that is null in Dash [8] in that no adsorption reactions are therein considered), convection (K_1, due to the velocity of the solute) and dispersion (K_2, which can be related to the Taylor's effective diffusivity as $D_{eff}=R_e^2 w_0^2 K_2/D_m$). While in Dash [8] a closed form solution was provided, in Nagarani [20],

due to the complexity of the equations involved, an exact solution was found for K_0 solely, whereas for K_1 and K_2 the asymptotic values were derived. It was seen that the asymptotic dispersion coefficient decreases with increase in the wall solute-absorption parameter β, and yield stress of the fluid (the GDM is in details recalled in the following of the paper).

The discussed methods and solutions strongly depend on the assumption that the transverse concentration distribution can be expanded in terms of eigenfunctions (Bessel functions for a circular pipe), that is properly verified only in the limit of complete transverse mixing. When the solute has not yet strongly interacted with the boundary, a free space expansion would be more suitable in describing the problem. Lighthill [19] first studied this transient and anomalous regime and found a solution for the concentration (that accounts for the transverse diffusion, but neglects longitudinal diffusion and interactions with the pipe's boundary) in terms of a Fourier transform, and showed that the tracer distribution, for small times, spreads longitudinally proportional to t (that is properly a superdiffusive behavior). Latini and Bernoff [18], more recently, have revisited the problem of dispersion of a point discharge of tracer in laminar pipe Poiseuille flow. Assuming a δ-function initial condition at the center of the pipe, and by means of a Fourier transform of the advection-diffusion equation, they fully modelled the three initial stages of dispersion, that is: (i) at small times, when diffusion dominates advection yielding a spherically symmetric Gaussian dispersion cloud; (ii) at large times, in correspondence of which the flow is in the classical Taylor regime and (iii) at an intermediate regime, where the longitudinal mean concentration profile is either asymmetric and anomalous.
Most recently, Decuzzi et al. [9] have extended the Taylor & Aris theory including the permeability of the walls to the sole solvent and leading to a new and more general expression for D_{eff} being

$$D_{eff} = D_m + \frac{v_0^2 R_e^2}{192 D_m}\left[\frac{\left(1+e^{2\zeta\Pi}\right)-e^{\Pi}\left(1+e^{2(\zeta-1)\Pi}\right)\Omega}{2-e^{\Pi}\left(1+e^{-2\Pi}\right)\Omega}e^{-\Pi\zeta}\right]^2 \tag{3}$$

with ζ the dimensionless longitudinal coordinate (=$D_m z/(R_e^2 v_0)$, where v_0 is the initial center line velocity), Π the permeability parameter and Ω the pressure parameter recalled in the following of the paper. The model proposed from Sharp has been subsequently refined by Gentile et al. [15], to introduce the effect of permeability of the channel to the solvent, inducing a reduction of velocity along the longitudinal coordinate as broadly discussed in Decuzzi et al. [9].

In the following, the generalized dispersion model re-proposed by Dash et al. [8] and Nagarani et al. [20] is combined with the steady-state solution given in [9] to analyze the unsteady dispersion of nanoparticles in permeable capillaries.

2. The mathematical model

A straight circular capillary with radius R_e and length l is considered (Fig. 1), the flow being described by a Newtonian fluid-law. The capillary walls may be permeable or impermeable to the fluid, but are impermeable and not adsorbent for the solute.

In the following the Generalized Dispersion Model is recalled and revised to consider the effective perfusion of the solvent through the walls. The dimensionless coefficients constituting the model are deducted and given in terms of the time and spatial variables, and of the permeability and pressure parameters Π and Ω, respectively. The relationship between the above cited coefficients and the effective diffusion coefficient D_{eff} is shown.

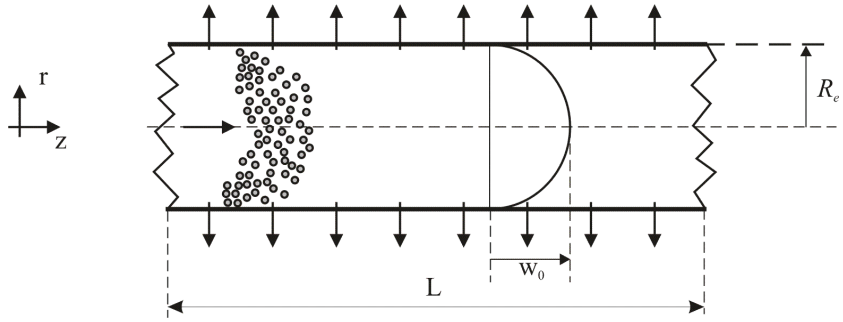

Fig. 1 The geometry of the channel where the nanoparticles are dislodged.

2.1 The Governing Equations

Following an approach firstly proposed by Sankarasubramanian and Gill [22], and more recently employed also by Dash et al. [8] and Nagarani et al. [20], the dispersion of a passive tracer or particles in a Poiseuille flow may be described in a dimensionless form by the advection-diffusion equation

$$\frac{\partial \psi}{\partial t} + \bar{v}\frac{\partial \psi}{\partial z} = \left(\frac{1}{r}\frac{\partial}{\partial r}\left(r\frac{\partial}{\partial r}\right) + \frac{1}{P_e^2}\frac{\partial^2}{\partial z^2}\right)\ \psi \tag{4}$$

expressed in terms of non dimensional physical quantities defined as

$$\psi = \frac{C}{C_0},\ \ \bar{v} = \frac{v}{v_0},\ \ \rho = \frac{r}{R_e},\ \ \zeta = \frac{D_m z}{R_e^{\,2} v_0},\ \ \tau = \frac{D_m t}{R_e^{\,2}} \tag{5}$$

where C and Ψ are the dimensional and non-dimensional concentration of the passive species respectively, C_0 is a concentration of reference, v_0 is the initial center line velocity, and v is the velocity distribution within the pipe given explicitly in the following paragraph, R_e is the radius of the capillary, D_m is the molecular diffusivity, r and z are the radial and longitudinal coordinates as from the frame of reference in Fig.1, and τ is the dimensional time variable. In (4) we used P_e (=$R_e v_0/D_m$) is the characteristic Peclet number. It is assumed that the particles are sufficiently small to have the same velocity of the dislodging fluid so that the diffusion/advection problem and the fluid-dynamic problem may be treated separately.

The solution for Ψ may be derived as (Gill et al. [16]; Dash et al. [8])

$$\psi = \sum_{i=0}^{\infty} f_i(\rho, \zeta;\ \tau)\frac{\partial^i \psi_m}{\partial \zeta^i} \tag{6}$$

where the parameters f_i are weight functions relating the local concentration Ψ to the derivative of order i of the mean concentration Ψ_m with respect to the spatial variable ζ (Notice that for i=0, (6) gives Ψ_m, with f_0=1). The mean concentration Ψ_m is averaged over the cross section as

$$\psi_m = 2\int_0^1 \psi \rho\, d\rho \tag{7}$$

and must obey the condition

$$\frac{\partial \psi_m}{\partial \tau} = \sum_{i=0}^{\infty} K_i(\zeta, \tau)\frac{\partial^i \psi_m}{\partial\ \zeta^i} \tag{8}$$

where the auxiliary functions $K_i(\zeta,, \tau)$ are given by

$$K_i(\zeta,\ \tau) = \frac{\delta_{i2}}{P_e^2} + 2\frac{\partial f_i}{\partial r}(1,\zeta;\ \tau) - 2\int_0^1 f_{i-1}(\rho,\ \zeta;\ \tau)\ \overline{v}(\rho,\ \zeta;\ \tau)\ \rho\ d\rho, \qquad f_{-1} = 0 \tag{9}$$

Here δ_{ij} denotes the Kronecker delta symbol.

Solving (8), with the appropriate initial and boundary conditions, the mean concentration $\Psi_m(\zeta, \tau)$ is derived and the local concentration $\Psi(\zeta, \rho; \tau)$ is eventually obtained using (6). Thus, the problem is basically reduced to estimating $f_i(\zeta, \rho; \tau)$ and $K_i(\zeta, \tau)$ for each i. For the weight functions $f_i(\zeta, \rho; \tau)$ a set of differential equations may be derived in a general form

$$\frac{\partial f_n}{\partial \tau} = \frac{1}{\rho}\frac{\partial}{\partial \rho}\left(\rho\frac{\partial f_n}{\partial \rho}\right) - \overline{v}(\rho,\ \zeta) f_{n-1} + \frac{1}{P_e^2} f_{n-2} - \sum_{i=0}^{n} K_i\ \ f_{n-i}, \qquad f_{-1} = f_{-2} = 0 \tag{10}$$

which relates $K_i(\zeta, \tau)$ and $f_i(\zeta, \rho; \tau)$. The equations (9) and (10) together with the initial and boundary conditions completely define the dispersion problem under analysis. It has also been shown by Sankarasubramanian and Gill that sufficiently accurate results are obtained by limiting the summation in (8) to the first three terms (i=2), that is

$$\frac{\partial \psi_m}{\partial \tau} = K_0 \Psi_m + K_1 \frac{\partial \psi_m}{\partial \zeta} + K_2 \frac{\partial^2 \psi_m}{\partial \zeta^2} + O\left(\frac{\partial^3 \psi_m}{\partial \zeta^3}\right) \tag{11}$$

and in the sequel higher order terms are neglected.

2.2 The Initial and Boundary Conditions

It is assumed that a bolus of particles at the time τ=0 is introduced instantaneously and uniformly along the radius ρ, thus to satisfy the initial condition

$$\psi_m(\zeta;\ 0) = \psi_{m0}(\zeta) \tag{12}$$

Note that no particular restrictions apply to the initial distribution profile of Ψ_m, i.e. the mean concentration at the initial time τ=0 may be the most general. On the other hand, since for τ=0 the solute is uniformly spread along every cross section of the channel, the local concentration has to satisfy the condition:

$$\psi(\rho,\ \zeta;\ 0) \equiv \psi_m(\zeta;\ 0) \tag{13}$$

It is further assumed that the pipe walls are impermeable to the particles constituting the solute,

$$\frac{\partial \psi}{\partial \rho}(1,\ \zeta;\ \tau) = 0 \tag{14}$$

while, due to the conservation of mass of the species diffusing in the channel, infinitely far away from the inlet section, the concentration as well as the derivatives of concentrations up to a generic order i go to zero

$$\psi(\rho,\infty;\ \tau) = \frac{\partial^i \psi}{\partial \rho^i}(\rho,\infty;\ \tau) = 0,\ \psi_m(\infty;\tau) = \frac{\partial^i \psi}{\partial \rho^i}(\infty;\ \tau) = 0 \tag{15}$$

and on the center line the symmetry condition imposes that

$$\psi\left(0,\ \zeta;\ \tau\right)=\text{finite and }\frac{\partial\psi}{\partial\rho}\left(0,\ \zeta;\ \tau\right)=0 \tag{16}$$

Considering (8) and (12)-(16), the initial and boundary conditions on Ψ and Ψ_m can be rephrased in terms of the weight functions f_i , leading to a new set of conditions which may be effective within the governing equations to derive explicit relations for K_i and f_i. In particular, from the definition of the average concentration (7), the solvability condition is straightforward derived as

$$\int_0^1 f_n\left(\rho,\ \zeta;\ \tau\right)\ \rho\, d\rho=\frac{\delta_{0n}}{2},\ \ n\geq 0 \tag{17}$$

where δ_{0n} is the Kronecker delta.

The initial condition of uniformity on Ψ can be analytically expressed through

$$\left.\frac{\partial\psi}{\partial\rho}\right|_{\tau=0}=0 \tag{18}$$

and, substituting (6) into (18):

$$f_n(\rho,\ \zeta;\ 0)\equiv f_n(\zeta;\ 0),\ \ n\geq 0 \tag{19}$$

From (19), (17) and (13) the initial conditions on the f_i are deducted as

$$f_n(\zeta;0)=\delta_{0n}, \tag{20}$$

while the boundary conditions are derived from (7), (14) and (16) as

$$\frac{\partial f_n}{\partial\rho}(1,\zeta;\tau)=0,\ \ \ n\geq 0, \tag{21}$$

and

$$f_n\left(0,\zeta;\tau\right)=\text{finite and }\frac{\partial f_n}{\partial\rho}\left(0,\zeta;\tau\right)=0,\ \ \ n\geq 0. \tag{22}$$

2.3 Solution for K_0 and f_0

The function f_0 and the exchange coefficient K_0 do not depend on the velocity field and can be solved directly. For n=0, eq. (9) reduces to

$$K_0(\zeta,\tau)=2\frac{\partial f_0}{\partial\rho}(1,\zeta;\tau), \tag{23}$$

that, through (21) allows for the determination of the exchange coefficient K_0 as

$$K_0(\zeta,\tau)=0. \tag{24}$$

Note that the coefficient K_0 is zero, therefore there are no absorption effects at the walls.

The function f_0 dictates the deviation of the local concentration Ψ from the mean concentration Ψ_m, due to solute absorption at the walls mechanisms. When there are no depletion effects of solute at the border, f_0 is set to one

$$f_0 = 1 \tag{25}$$

which is the sole solution of (110) that satisfies both the boundary conditions (21) and (22) and the initial condition (20). This may be proved as follows: from (10), imposing n=0, the expression

$$\frac{\partial f_0}{\partial \tau} = \frac{1}{\rho}\frac{\partial}{\partial \rho}\left(\rho \frac{\partial f_0}{\partial \rho}\right) \tag{26}$$

is obtained. Using the solvability condition (17) in (26), the expressions

$$\frac{\partial f_0}{\partial \rho} = 0, \quad \forall \tau, \tag{27}$$

$$\frac{\partial f_0}{\partial \tau} = 0, \quad \forall \rho \tag{28}$$

may be derived, which, together with (20), allow for the deconvolution of f_0 as f_0=1.

2.4 Solution for K_1 and f_1

For n=1, Eq. (10) becomes

$$\frac{\partial f_1}{\partial \tau} = \frac{1}{\rho}\frac{\partial}{\partial \rho}\left(\rho \frac{\partial f_1}{\partial \rho}\right) - v(\rho,\ \zeta) - K_1, \tag{29}$$

recalling that f_{-1}=0. Multiplying (29) by ρ and integrating from 0 to 1 with respect to ρ, along with the solvability condition (17), it follows that

$$K_1(\zeta) = -2\int_0^1 \overline{v}(\rho,\zeta)\ \rho\, d\rho \equiv -\overline{v}_m(\zeta). \tag{30}$$

If the conduit is impermeable then the velocity profile depends on the radius solely and it may be described by the classical Poiseuille parabolic velocity distribution. It follows that $K_1(\zeta)\equiv -0.5$ (as obtained in Dash [8]).

The distribution function f_1 is a solution for the partial differential equation (29); that can be decomposed (Dash [8]; see also Gill and Sankarasabrumanian [17]; Nagarani et al. [20] as

$$f_1(\rho,\zeta;\tau) = f_{1s}(\rho,\zeta) + f_{1t}(\rho,\zeta;\tau), \tag{31}$$

where $f_{1s}(\rho, \zeta)$ is the steady state solution, whereas $f_{1t}(\rho, \zeta; \tau)$ is the transient, time-dependent solution. Following an approach as in Dash [8], the expressions for f_{1s} and f_{1t} may be derived as

$$f_{1s}(\zeta,\rho) = \overline{v}_0(\zeta)\left(\frac{1}{8}\rho^2 - \frac{1}{16}\rho^4 - \frac{1}{24}\right), \tag{32}$$

where $\overline{v}_0(\zeta)$ is the non-dimensional centerline velocity of the flow and

$$\begin{aligned} f_{1t}(\rho,\zeta;\tau) &= \sum_{n=0}^{\infty} -\frac{2\int_0^1 J_0(\lambda_n\rho) f_{1s}(\rho,\zeta)\ \rho\, d\rho}{\left[J_0(\lambda_n)\right]^2} e^{-\lambda_n^2\tau} J_0(\lambda_n\rho) = \\ &= \sum_{n=0}^{\infty} -\frac{2\int_0^1 J_0(\lambda_n\rho)\overline{v}_0(\zeta)\left(\frac{1}{8}\rho^2 - \frac{1}{16}\rho^4 - \frac{1}{24}\right)\ \rho\, d\rho}{\left[J_0(\lambda_n)\right]^2} e^{-\lambda_n^2\tau} J_0(\lambda_n\rho), \end{aligned} \tag{33}$$

the eigen values λ_n as the roots of the equation $J_1(\lambda_n)=0$. Note that for impermeable channels (where the non-dimensional center line velocity is constant ad given by $\overline{v}_0(\zeta)\equiv 1$ eqs. (32) and (33) are deducted as

$$f_{1s}(\rho)=\frac{1}{8}\rho^2-\frac{1}{16}\rho^4-\frac{1}{24}, \tag{34}$$

$$f_{1t}(\rho;\tau)=\sum_{n=0}^{\infty}-\frac{2\int_0^1 J_0(\lambda_n\rho)\left(\frac{1}{8}\rho^2-\frac{1}{16}\rho^4-\frac{1}{24}\right)\rho\,d\rho}{\left[J_0(\lambda_n)\right]^2}e^{-\lambda_n^2\tau}J_0(\lambda_n\rho), \tag{35}$$

These results coincide with those derived by Dash [8], provided that the plug radius r_p is null (meaning that the Casson Fluid degenerates into Newtonian).

2.5 Solution for K_2

To derive the expression for K_2, the same approach as for K_0 and K_1 is used. Imposing n=2 within (10), multiplying by ρ ad integrating from 0 to 1, after some algebra the expression for K_2 is obtained as

$$K_2(\zeta,\tau)=\frac{1}{P_e^2}-2\int_0^1 f_1\,\overline{v}(\rho,\zeta)\,\rho\,d\rho, \tag{36}$$

which may be simplified in

$$K_2(\zeta,\tau)=\frac{1}{P_e^2}+\frac{\overline{v}_0(\zeta)}{192}-2\int_0^1 f_{1t}\,\overline{v}(\rho,\zeta)\,\rho\,d\rho. \tag{37}$$

Note that in the limit of $\tau\to\infty$ the classical solution by Taylor and Aris can be recalled, where the effective longitudinal diffusion coefficient D_{eff} is given as

$$D_{eff}=\frac{R_e{}^2 v^2{}_0(\zeta)}{D_m}K_2 \tag{38}$$

whereas in general D_{eff} would depend also on time τ.

It is here important to note that, in the original formulation by Gill and Sankarasubramanian [17], where for the first time the idea of a time-dependent effective diffusion was introduced, the auxiliary functions K_i were only depending on time τ. Differently in the present formulation, the fluid velocity is no more constant along the capillary because of its lateral permeability which induces a continuous reduction in flow velocity with ζ. Consequently, the auxiliary functions K_i would in general depend on ζ too. And, in particular, the problem would be determined if the velocity field in the capillary is known.

2.6 The velocity distribution (effect of boundary depletion of the solvent)

Recalling the dimensionless variables (5) and introducing the non dimensional pressure

$$p=\underline{p}D_m/\left(4\mu v_0^2\right) \tag{39}$$

the classical governing equation for the laminar flow in a circular pipe of radius R_e is given by

$$\rho\frac{\partial p}{\partial\zeta}=\frac{1}{4}\frac{\partial}{\partial\rho}\left(\rho\frac{\partial\overline{v}}{\partial\rho}\right), \tag{40}$$

with μ being the dynamic viscosity of the fluid and $\underline{p}$ the dimensional pressure within the capillary. Imposing the no-slip condition at the wall ($\overline{v}$ (1, ζ)=0 and the symmetry condition at the center line ($\partial \overline{v}(0,\rho)/\partial\rho=0$), with the assumption that the gradient of pressure along the longitudinal direction is constant, the classical Poiseuille parabolic velocity distribution is readily recovered as

$$\overline{v}(\rho,\zeta) = -\left(1-\rho^2\right)\frac{dp}{d\zeta}, \tag{41}$$

from which the non-dimensional centerline velocity $v_0(\zeta)$ is derived:

$$\overline{v}_0(\zeta) = \overline{v}(0,\zeta) = -\frac{dp}{d\zeta}; \tag{42}$$

while the dimensional mean velocity v_m is given by

$$V = \frac{1}{\pi \mathrm{R}_e^2}\int_0^{\mathrm{R_e}} v(r,z)\ 2\pi r dr = \frac{2}{\mathrm{R}_e^2}\int_0^{\mathrm{R_e}} v(r,z)\, r dr \tag{43}$$

and the non dimensional mean velocity $\overline{v}_m$

$$\overline{v}_m = 2\int_0^1 \overline{v}(\rho,\zeta)\,\rho d\rho = 2\int_0^1 -\left(1-\rho^2\right)\frac{dp}{d\zeta}\,\rho d\rho = -\frac{1}{2}\frac{dp}{d\zeta}. \tag{44}$$

If the walls of the capillary are permeable to the solvent, there would be fluid leaking across the walls leading to a continuous reduction of the flow rate along the channel. Still assuming that the fluid lateral flux does not modify the velocity profile within the channel which still obeys to the Poiseuille parabolic distribution, i.e. the hypothesis of mono-dimensional flow still holds true. Mass continuity for an incompressible flow imposes that

$$\frac{\partial Q}{\partial z} + v_p \lambda_p = 0, \tag{45}$$

where Q is the volume flow rate, defined as

$$Q = \int_0^{\mathrm{R_e}} v\ 2\pi r dr = V\pi R_e^2\ , \tag{46}$$

that, in non-dimensional terms, has the form:

$$\Theta = \int_0^1 \overline{v}\ 2\pi\rho d\rho = -\frac{\pi}{2}\frac{dp}{d\zeta}, \tag{47}$$

while $\lambda_p=2\pi R_e$ is the lateral profile of the wall, and v_p the perfusing velocity derived from Darcy's law as

$$v_p = -L_p(\pi_i - \underline{p}); \quad L_p = \frac{k}{\mu\,\delta} \tag{48}$$

where L_p is the vascular hydraulic conductivity expressed as a function of the lateral thickness δ and the permeability k of the capillary wall; π_i is the interstitial fluid pressure (IFP). The mass continuity can be then rephrased in non-dimensional terms as

$$\frac{\partial\Theta}{\partial\zeta} - L_p(\pi_i - p) = 0 \tag{49}$$

which, through (47), allows to obtain the partial differential equation that dictates the change in pressure along the channel (whose length is l)

$$\frac{\partial^2 p}{\partial \zeta^2}+\left(\frac{\Pi}{\zeta_l}\right)^2(1-p)=0;\quad p=\frac{p}{\pi_i},\quad \zeta_l=\frac{l\times D_m}{R_e^2 v_0},\quad \Pi=\zeta_l\sqrt{\frac{2\hat{L}_p}{\pi}}; \tag{50}$$

provided that the followings hold true

$$\Theta=\frac{Q}{v_0 \mathrm{R}_e^2}, \tag{51}$$

$$\hat{L}_p=8\pi R_e^2\frac{L_p}{D_m^2}v_0^2\mu\,. \tag{52}$$

Solving with the boundary conditions

$$\begin{aligned} p(0)&=p_0 \text{ inlet pressure}\\ p(\zeta_l)&=p_1 \text{ outlet pressure}\end{aligned} \tag{53}$$

the pressure distribution along the channel is finally derived as

$$\begin{aligned} p(\zeta)=\frac{1}{2}[&\left(-e^{(\zeta_l-\zeta)\Pi/\zeta_l}+e^{(\zeta+\zeta_l)\Pi/\zeta_l}\right)(p_1-1)+\\ &+\left(e^{2(\zeta_l-\zeta)\Pi/\zeta_l}-e^{\zeta\Pi/\zeta_l}\right)(p_0-1)+e^{2\Pi}-1]\left(\coth[\Pi]-1\right).\end{aligned} \tag{54}$$

The effective velocity distribution may be finally obtained as

$$\begin{aligned} \bar{v}(\rho,\zeta)&=\frac{-\pi_i\frac{dp}{d\zeta}\left(1-\rho^2\right)}{-\pi_i\frac{dp}{d\zeta}\Big|_{\zeta=0}}\\ &=e^{-\zeta\Pi/\zeta_l}\times\\ &\times\frac{\left[e^{\Pi}(p_1-1)+e^{(\zeta_l+2\zeta)\Pi/\zeta_l}(p_1-1)-e^{2\Pi}(p_0-1)-e^{2\zeta\Pi/\zeta_l}(p_0-1)\right]}{2e^{\Pi}(p_1-1)-(p_0-1)(1+e^{2\Pi})}\\ &\times(1-\rho^2)\\ &=e^{-\zeta\Pi/\zeta_l}\frac{\left[1+e^{2\zeta\Pi/\zeta_l}-\Omega\left(1+e^{2(\zeta-\zeta_l)\Pi/\zeta_l}\right)e^{\Pi}\right]}{2-e^{\Pi}(e^{-2\Pi}+1)\Omega}(1-\rho^2),\end{aligned} \tag{55}$$

Where$\Omega=(p_0-\pi_i)/(p_1-\pi_i)$ is the pressure parameter, while Π is the permeability parameter as defined in (50). From (55) it stems out that the permeability of the walls does not modify the Poiseuille characteristic velocity profile along the cross section of the capillary; nevertheless it induces a reduction in velocity along ζ. In consideration of these results, the variables of the model of diffusion can be determined, and shown in the following.

3. Results

3.1 The diffusive term

As shown in (38), the diffusive term K_2 is proportional to the effective diffusion coefficient. In an impermeable capillary, the diffusive term K_2 grows with time along the capillary as shown by Gill and Sankarasubramanian [16]. This is shown in Fig.2, which gives the contour plot of K_2 as a function of time τ (0, 0.5) and position along the capillary ζ (0, 1). Note that as time increases, the solution for K_2 tends to a constant asymptotic value coinciding with that of Taylor & Aris.

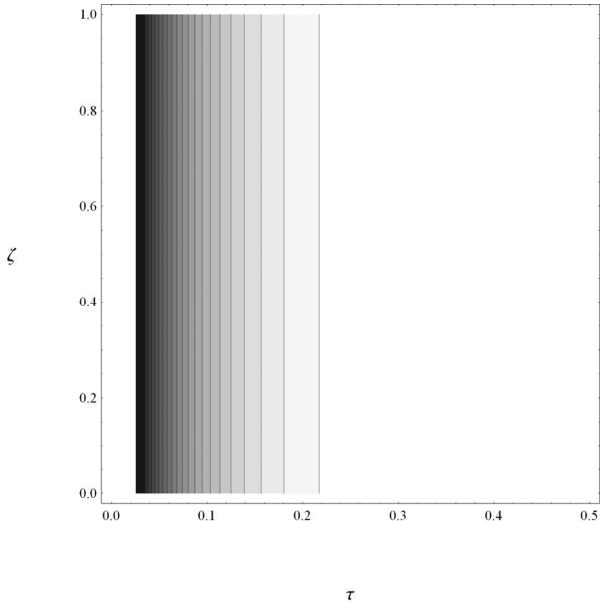

Fig. 2. K_2 ContourPlot ($\zeta \in [0,1]$, $\tau \in [0,0.5]$, $\Pi=0$, $\Omega=-2$).

In Fig.3, the same contour plot is shown for a non zero capillary wall permeability ($\Pi=2$). As predicted in [9], the effective diffusion coefficient D_{eff}, and thus K_2, is not uniform along the capillary: it reduces from the inlet of the capillary, reaches a minimum value and then increases again as the outlet of the capillary is approached. And this same behavior is shown at each time interval. Again it is verified that the asymptotic solution, in this case coinciding with that derived in [9] is reached after a sufficiently large time $\tau>0.5$. As Π increases, the variation of K_2 along the capillary becomes steeper and a central area of the capillary can be identified where the beneficial effect of the convection on the longitudinal dispersion of the solute particles is null.

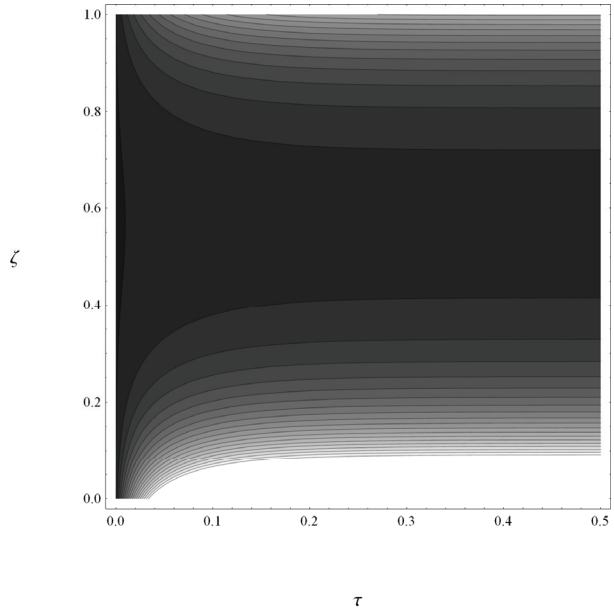

Fig. 3. K_2 ContourPlot ($\zeta \in [0,1]$, $\tau \in [0,0.5]$, $\Pi=2$, $\Omega=-2$).

3.2 The local dimensionless concentration Ψ

The local concentration Ψ is derived according to (6) truncated at the first order and is shown in Fig.4 as a function of the dimensionless radius ρ and longitudinal coordinate ζ, at the time $\tau=0.4$. The permeability parameter Π is null ($\Pi=0$) meaning that the results are herein shown for an impermeable capillary.

To some extent the concentration resembles a wave with its front travelling faster downstream along the centerline of the capillary, and its tails following the peak of concentration with some delay. This is due to the non-uniform velocity profile along ρ showing a maximum at $\rho=0$ (center of the capillary) and being instead zero at $\rho=1$ (boundary of the capillary). As a consequence, the bolus of nanoparticles either (i) cluster around the centerline or (ii) aggregate near the borders of the channel, depending on the particular cross section under study (downstream with respect to the peak of concentration ($\Psi_{m,max}$) the first behavior is observed). Notice that this mechanism is mathematically described within (6) by the term f_1 times $\partial \Psi_m/\partial\zeta$: when the mean concentration attains a maximum, that is $\partial \Psi_m/\partial\zeta=0$, then $\Psi \equiv \Psi_m$ regardless the transverse coordinate ρ, elsewhere the function f_1 dominates, and Ψ would be in general different from Ψ_m.

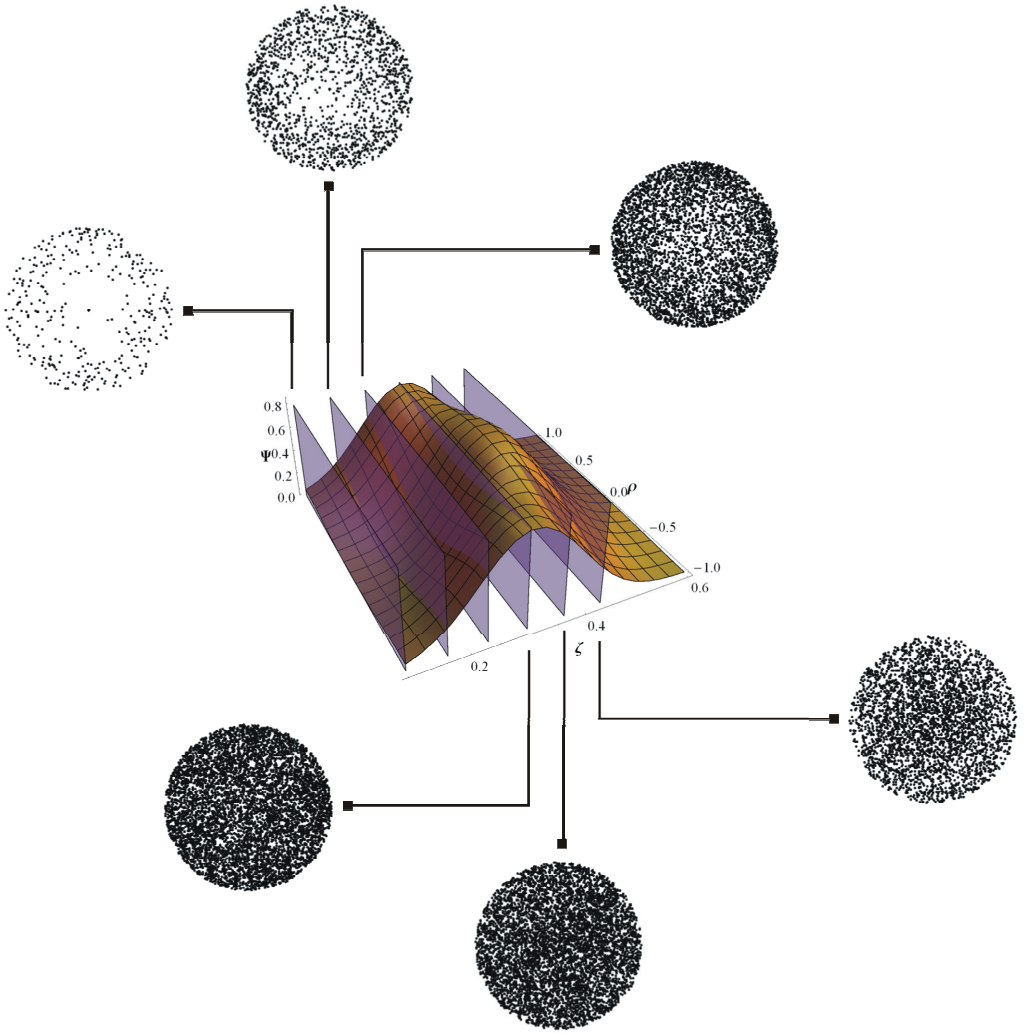

Fig. 4. The local concentration Ψ (τ=0.4; Π=0).

The function f_1 depends, among others, on the centerline velocity v_0 along ζ, that means that a change in Π or Ω would locally affect the local concentration as well. The effect of permeability is investigated in Figs. 5 and 6, where the local concentration Ψ is shown versus ζ and ρ at a fixed time (τ=0.4) and for different values of Π (=1, 5). As Π increases, the concentration gets more and more peaked, in that K_2 reduces inducing a general delay in the redistribution of the nanovectors in the capillary (the dispersion that the solute experiences along ζ is due to the non uniform velocity profile of the flow, and described in non dimensional terms by K_2). Also, at the limit of high Π any gradient of concentration along ρ would be canceled, meaning that the particles constituting the solute would be uniformly distributed over each cross section of the capillary. This is evidently due to permeability via the shape function f_1 – the perfusion of the solvent through the walls modifies the velocity along ζ, contributing to redistribute the concentration and reshape the distribution of solute in the capillary, thus strongly reducing the gradients of concentration along the radius ρ. In Fig.6 (Π=5) the particles are prevalently clustered around the centroid of the distribution, and show no preferential

orientation along the radius; whereas in Fig.5 (Π=1) and Fig.4 (Π=0) these effects are far less pronounced.

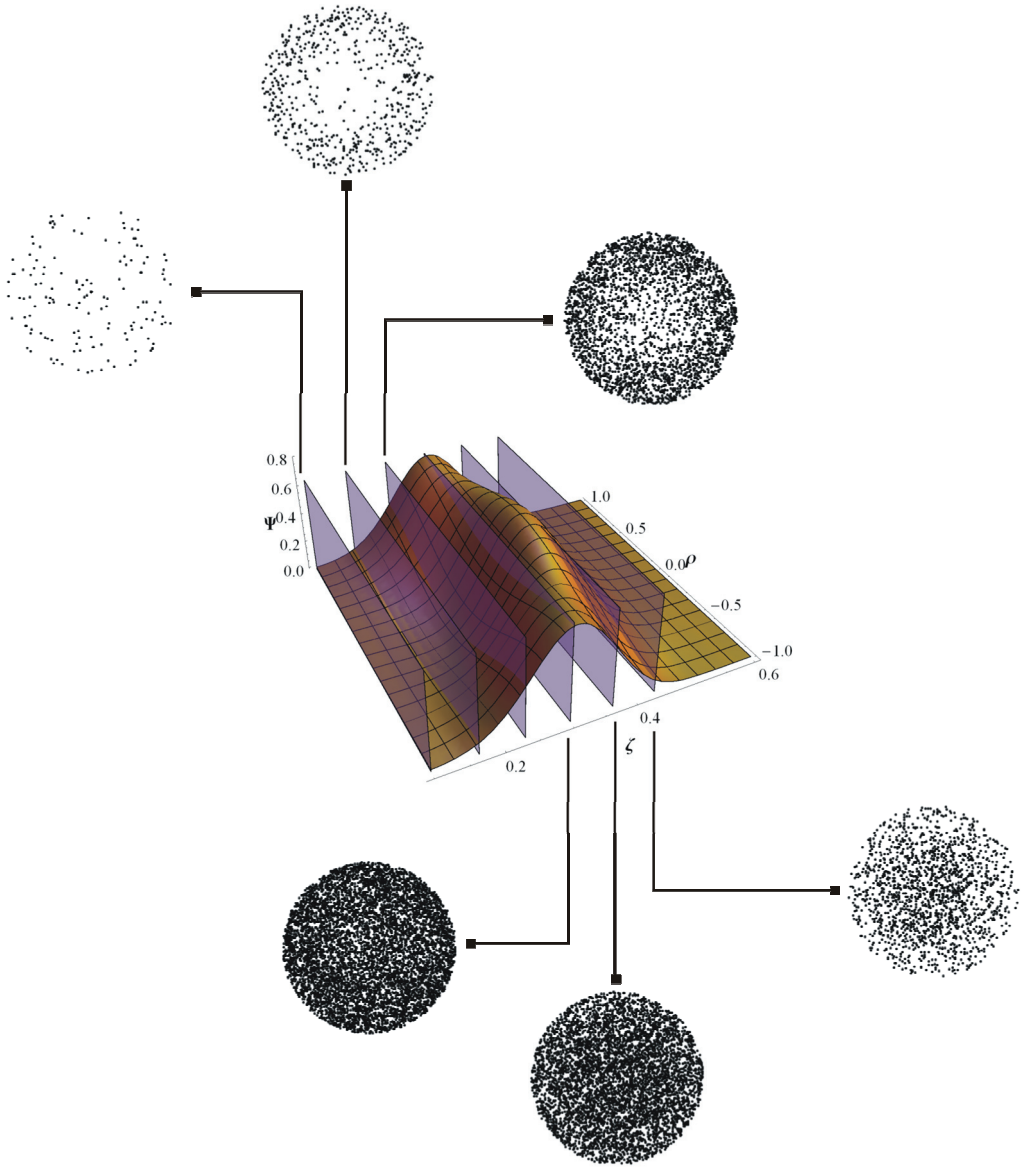

Fig. 5. The local concentration Ψ (τ=0.4; Π=1; Ω=–2).

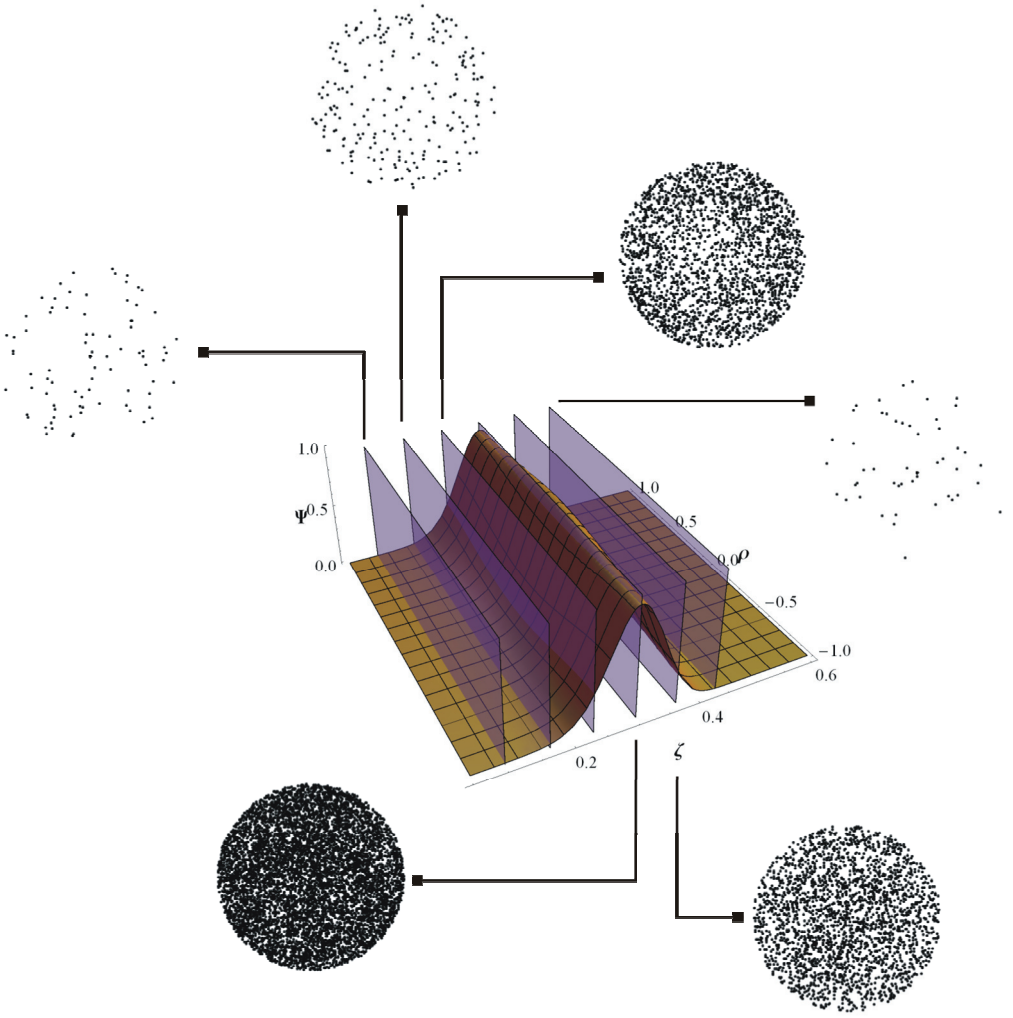

Fig. 6. The local concentration Ψ (τ=0.4; Π=5; Ω=–2).

Fig.7 illustrates the shape function f_1 versus ρ at different values of permeability (Π=0, 1, 5; Ω=–2), and different cross sections ζ (ζ=0, 0.2, 0.5, 0.8), time parameter being hold constant as τ=0.5. The higher the values of permeability, the lower the modulus of f_1 everywhere in the channel, and less sensible the differences between the local and average concentration. Notice that at the center of the channel (where the fluid is most likely stagnant) these effects are more dramatic, whereas in the close proximity of the inlet they are negligible, up to be null at the limit $\zeta \to 0$ (at the entrance of the channel the function f_1 is invariant whatever the value of permeability Π).

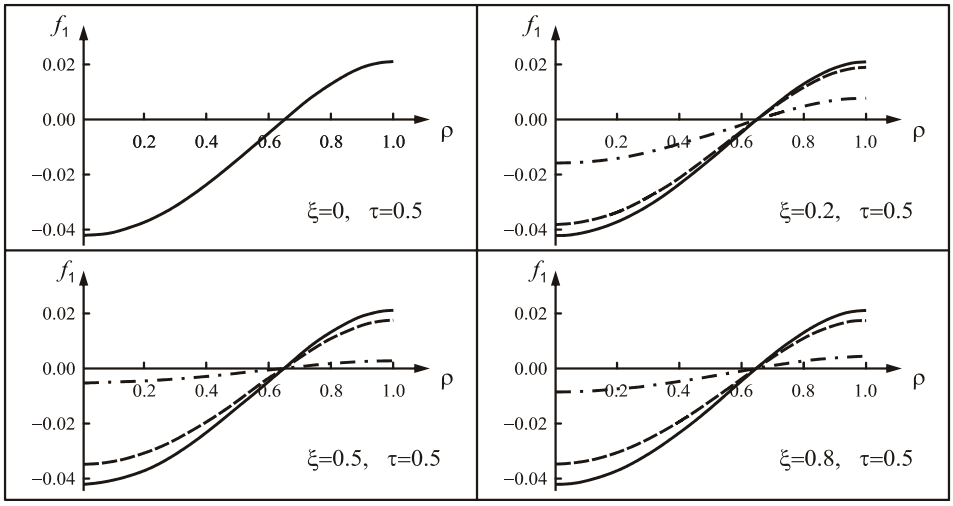

Fig. 7. The shape function f_1 versus the radius ρ at different cross sections (τ=0.5; Ω=–2; solid lines: Π=0; dashed lines: Π=1; dashed-dotted lines: Π=5).

4. Conclusions

Stemming from the generalized dispersion model (Gill et al. [16], Dash et al. [8], Nagarani et al. [20]), the unsteady dispersion of a solute in a permeable channel was derived in terms of the dimensionless effective diffusion coefficient K_2. It was found that for a given set of permeability parameters different from zero, K_2 increases with time up to a value that depends on the position ζ within the channel, and that can never be higher than the theoretical limit $K_{2,max}=D_{eff0}\times D_m/R_e^2 v_0^2$ where D_{eff0} is the Taylor and Aris diffusion coefficient derived at the entrance of the channel. In general, K_2 would be lower in the central regions of the capillary, where the velocity of the fluid dramatically reduces, and the higher the permeability, the smaller the dimensionless diffusion coefficient. Nevertheless, whatever the longitudinal coordinate ζ, or the permeability parameters Π and Ω, the time employed to reach the steady state regime is the same ($\tau_{steady}=0.5\times R_e^2/D_m$), meaning that an increased leakage would not modify the coefficients K_1 and K_2 in time (but through K_1 and K_2 the bolus of solute would experience different histories of dispersion). Most important, it was found that the perfusion of the solvent at the walls would uniformly redistribute the concentration along the radius of the channel.

As discussed in Decuzzi et al. [9], and Gentile et al. [15], in a network of capillaries a solute would most likely follow the path presenting the largest effective diffusivity. Based on these theoretical findings it may be concluded that a bolus of nanovectors would preferentially move in larger vessels (where high Reynolds number flows occur, V=O(1 mm/s)) rather than in small, leaky capillaries of the tumor districts (with small blood velocities, V=O(100 μm/s) or less). Also, the quasi uniform radial distribution of the solute in permeable capillaries represents a novel biological barrier. Margination and extravasation of nanovectors is in fact hindered (or, at least, it is not favoured), and only a small amount of such nanocarriers (those in close proximity of the walls) would be candidate to sediment on the surface and extravasate.

However, the analysis presented so far is approximate in that it relies on the strong assumption that the particles are sufficiently small to have the same velocity of water molecules: as it stands, this approach completely disregards the physical, chemical and

geometrical properties of the nanovectors constituting the solute. Considering the above mentioned properties is equivalent to introducing into the problem more degrees of freedom that may be suitably tailored to severally enhance the performance of these nanocarriers. For instance, in recent experiments [14] it was shown that in a flow chamber system and under the influence of a gravitational field, the number of marginating particles over time increases if discoidal or quasi-hemispherical particles are used in place of spheres. And that would demonstrate that non-spherical inertial particles would perform better than classical spherical, pertaining drug delivery and bio-imaging.

References

[1] A.I. Minchinton and I.F. Tannock, Drug penetration in solid tumors, Nature Reviews Cancer, 2006; 6; 583-592;
[2] M. Ferrari; Nanovector therapeutics, Current opinion in Chemical Biology; 2005; 9; 343-346.
[3] Li, K. C. P., Pandit, S. D., Guccione, S., Bednarski, M. D. Molecular imaging applications in nanomedicine. Biomed. Microdevices 6, 113–116 (2004)
[4] C-H Heldin, K. Rubin, K. Pietras and A. Ostman; High Interstitial fluid pressure – an obstacle in cancer therapy, Nature Reviews Cancer, 2004; 4; 806-813
[5] Ananthakrishnan V., W. N. Gill and A. J. Barduhn, Laminar dispersion in capillaries: Part I. Mathematical analysis, *AIChE J.* 11:1063-1072, 1965.
[6] Aris R., On the dispersion of a solute in a fluid flowing through a tube, *Proc. R. Soc. Lond. A* 235(1200):67–77, 1956.
[7] Carslaw H. S. and Jaeger J. C., Conduction of Heat in Solids, *Clarendon Press*, Oxford, 1959 (second edition).
[8] Dash R. K., Jayaraman G. and Mehta K. N., Shear-Augmented Dispersion of a Solute in a Casson Fluid Flowing in a Conduit, *Ann. Biomed. Eng.* 28:373-385, 2000.
[9] Decuzzi P., Causa F., Ferrari M. and Netti P. A., The Effective Dispersion of Nanovectors Within the Tumor Microvasculature, *Ann Biomed Eng.*, 34(4):633-641, 2006.
[10] Fahraeus R., 1929, The Suspension Stability of the Blood, *Physiol. Rev.*, 9, 241-274.
[11] Ferrari M., Cancer Nanotechnology: opportunities and challenges, *Nature Reviews Cancer*, 2005; (5):161-171.
[12] Fung Y.C., Biomechanics, *Springer*, New York, 1990.
[13] Ganong, W. F. Review of Medical Physiology, 21st ed. New York: *Lange Medical Books/McGraw-Hill*, Medical Publishing Division, 2003.
[14] Gentile F., Chiappini C., Fine D., Bhavane R.C., Peluccio M.S., Ming-Cheng Cheng M., Liu X., Ferrari M.and Decuzzi P., The Margination Dynamics of non Spherical Inertial Particles in a MicroChannel, *Journal of Biomechanics*, under review. 2007
[15] Gentile F., Ferrari M. and Decuzzi P., The Longitudinal Transport of Nanoparticles within a Casson Fluid in a Permeable Capillary, *Annals of Biomedical Engineering*, in print, 2007.
[16] Gill W. N, A note on the solution of transient dispersion problems, *Proc. R. Soc. London*, Ser. A 298:335-339, 1967.
[17] Gill W. N. and R. Sankarasubramanian, Exact analysis of unsteady convective diffusion, *Proc. R. Soc. London*, Ser. A, 316:341-350, 1970.
[18] Latini M. and Bernoff A. J., Transient Anomalous Diffusion in Poiseuille Flow, *J. Fluid Mech.*, 441:399-411, 2001.
[19] Lighthill M. J., Initial Development of Diffusion in Poiseuille Flow, *J. Inst. Maths. Appl.* 2:97-108, 1966.

[20] Nagarani P., Sarojamma G. and Jayaraman G., Effect of Boundary Absorption in Dispersion in a Casson Fluid Flow in a Tube, *Ann. Biomed. Eng.* 32:706-719, 2004.
[21] Phillips C. G. and Kaye S. R., The Initial Transient of Concentration During the Development of Taylor Dispersion, *Proc. R. Soc. London*, Ser. A, 453:2669-2688, 1997.
[22] Sankarasubramanian R. and Gill W. N., Unsteady Convective Diffusion with Interphase Mass Transfer, *Proc. R. Soc. London*, Ser. A 333:115-132, 1973.
[23] Sharp M. K., Shear-augmented dispersion in non-Newtonian fluids, *Ann. Biomed. Eng.* 21:407-415, 1993.
[24] Siegel P., Mosè R., Ackerer P. H. and Jaffre J., Solution of the Advection-Diffusion Equation Using a Combination of Discontinuous and Mixed Finite Elements, *International Journal for Numerical Methods in Fluids* 24:595-613, 1997.
[25] T. Lindquist, 1931., The Viscosity of the Blood in Narrow Capillary Tubes, *Am. J. PhysioL*, 96, 562-568.